Chemical Engineering Journal 163 (2010) 422–428

Contents lists available at ScienceDirect

Chemical Engineering Journal

journal homepage: www.elsevier.com/locate/cej

Kinetic study on the synthesis of ethyl nitrite by the reaction of C_2H_5OH, O_2, and NO in a trickle bed reactor

Huajun Wang[a], Guangxing Li[b,*]

[a] School of Chemistry and Chemical Engineering, Huazhong University of Science and Technology, Wuhan 430074, PR China
[b] Hubei Key Laboratory of Material Chemistry & Service Failure, Huazhong University of Science and Technology, Wuhan 430074, PR China

ARTICLE INFO

Article history:
Received 11 January 2010
Received in revised form 21 July 2010
Accepted 26 July 2010

Keywords:
Ethyl nitrite
Synthesis
Trickle bed reactor
Kinetics
Two-film model

ABSTRACT

The synthesis of ethyl nitrite by the reaction of C_2H_5OH, O_2, and NO, called the regeneration reaction in the synthesis of ethylene glycol (EG) by the coupling reaction-hydrogenation process, is carried out in a trickle bed reactor filled with θ-mesh rings at 313–343 K and atmospheric pressure. It is shown that the conversion of O_2 increases with the NO/O_2 and the EtOH/NO molar ratios, and decreases with the N_2 volume fraction and the liquid hourly space velocity (LHSV). O_2 conversion reaches a maximum (~90.9%) at 333 K, NO/O_2 molar ratio of 6:1, EtOH/NO molar ratio of 3:1, N_2 volume fraction of 50%, and LHSV of 2.65 h^{-1}. The synthesis reaction is a fast one and takes place in a liquid film. A kinetics model based on the two-film model of gas–liquid reaction is proposed. The experiment data fit the kinetics model very well and statistical tests also show their reliability.

1. Introduction

Ethylene glycol (EG) is an important material for the synthesis of many kinds of chemicals, such as polyester fiber, antifreeze, and so on. Commercially, it is synthesized by the hydration of ethylene oxide, which is produced in the petrochemical industry. Taking into account the current shortage of petroleum resources, many efforts have been made to develop new and alternative processes for the synthesis of EG. Among these approaches, the Ube process, which is based on C1 chemistry, is a promising one [1–3]. In this process, EG is synthesized by the hydrogenation of diethyl oxalate (DEO), which is produced from the catalytic coupling reaction of ethyl or methyl nitrite (EN/MN) and carbon monoxide. In the catalytic coupling process, two chemical reactions, including the coupling reaction (1) and the regeneration reaction (i.e. the synthetic reaction of EN) (2), take place simultaneously as follows [2]:

$$2CO + 2C_2H_5ONO \rightarrow (COOC_2H_5)_2 + 2NO \quad (1)$$

$$O_2 + 4NO + 4C_2H_5OH \rightarrow 4C_2H_5ONO + 2H_2O \quad (2)$$

In the coupling reaction, EN produced in the regeneration reaction reacts with carbon monoxide to form DEO, while in the regeneration reaction, NO produced in the coupling reaction reacts with EtOH and O_2 to form EN. Studies on the catalysis of the coupling reaction (1) and the hydrogenation of DEO have attracted increased attention [4,5]. Studies on the regeneration reaction (2), however, have not been studied in detail.

Generally, the regeneration reaction (2) is carried out in either a bubble column reactor or a distillation column reactor [6–8]. In these reactors, however, the feed amount of EtOH is much larger than the stoichiometry of the other reactants and some disadvantages are found: the purification of EtOH is very complicated due to the formation and accumulation of byproducts, such as ethanal, nitric acid, and water; furthermore, the running for the cycle processes of the coupling-regeneration reaction is unfavorable due to the solution of EN in EtOH. Chen [9] studied the kinetics of the regeneration reaction in a bubble column reactor and pointed out that the liquid drop type or liquid film type reaction model was suitable for the regeneration reaction. Considering that, in the trickle bed reactor, the accumulation of byproducts in the EtOH solution can be avoided, Li [10] suggested the use of the trickle bed reactor for the regeneration reaction.

The regeneration reaction is a gas–liquid heterogeneous reaction without any catalyst. The relationship between the reaction rate and mass transfer is very complicated. The mass transfer between the gas and liquid phases is the controlling step for the fast reaction [11,12]. The kinetics of the regeneration reaction is necessary for the design of the trickle bed reactor. However, the kinetics published in the literature so far is for regeneration reactions in a bubble column reactor at temperature ranges of 288–333 K [9]. The mass transfer behaviors of reactants in a bubble column reactor are significantly different from those in a trickle bed reactor

Abbreviations: DEO, diethyl oxalate; EG, ethylene glycol; EN, ethyl nitrite; EtOH, ethanol; LHSV, liquid hourly space velocity (h^{-1}); GHSV, gas hourly space velocity (h^{-1}); RE, relative error.

* Corresponding author. Tel.: +86 27 87543732; fax: +86 27 87543632.
E-mail address: ligxabc@163.com (G. Li).

1385-8947/$ – see front matter © 2010 Elsevier B.V. All rights reserved.
doi:10.1016/j.cej.2010.07.055

Nomenclature

a	effective gas–liquid interfacial area (m^2/m^3)
C_i	molar concentration of component i in liquid phase (mol/m^3)
C_{AG}, C_{BG}	molar concentration of O_2 and NO in gas phase, respectively (mol/m^3)
C_{CL}	liquid bulk concentration of EtOH (mol/m^3)
D_{LA}, D_{LB}	diffusion coefficient of O_2 and NO in liquid, respectively (m^2/s)
F	F-test function
F_T	tabulated value of F distribution
G	gas flow rate, m^3/s, in Eq. (26)
G'	gas flow rate, $kmol/(m^2\,s)$, in Eq. (20)
H_A, H_B	Henry's constant of O_2 and NO, respectively ($Pa\,m^3/mol$)
Ha	Hatta number, defined by Eq. (17)
$\Delta_r H_m^\theta$	standard molar enthalpy of reaction (kJ/mol)
h	height of the θ-mesh rings packing bed (m)
k	reaction rate constant ($m^6/(mol^2\,s)$)
k_{LA}	mass transfer coefficient of liquid film (m/s)
L	liquid flow rate (m^3/s), in Eq. (26)
L'	liquid spray density ($m^3\,m^{-2}\,h^{-1}$), in Eq. (19)
M_B	molar mass of solvent B (g/mol)
N	number of experimental runs
N_A	mass transfer rate ($mol/(m^2\,s)$)
p	number of parameter
R_A	reaction rate ($mol/(m^3\,s)$)
R	gas constant, 8.314 J/(mol k)
T	temperature (K)
u_{OG1}	gas inlet flow rate (m/s)
V_A	molecular volume of solute A at normal boiling point (cm^3/mol)
X_A	conversion of O_2 (%)
y_i	molar fraction of component i
z	coordinate

Greek letters

β	enhancement factor
δ_R, δ_L	thickness of reaction film and liquid film, respectively (m)
μ	liquid viscosity (mPa s)
ν_i	stoichiometric coefficient of component i
σ_A	expansion factor to component A
ψ	objective function

[13,14]. As such, the kinetic behavior obtained in the bubble column reactor is not suitable for use in the trickle bed reactor. In this work, experiments were carried out in a trickle bed reactor filled with θ-mesh rings to investigate the effects of the operation parameters. The kinetic model of the regeneration reaction based on the two-film model in the trickle bed reactor was established. The rate parameters of the kinetic model are determined by fitting the model predictions to the experiments.

2. Experimental

2.1. Materials

The NO (Tianjin Summit Specialty Gases Co., Ltd., Tianjin, China) used was of 99.9% purity. The purities of both O_2 and N_2 (Wuhan Ming Hui Gas Technology Co., Ltd., Wuhan, China) were 99.999%. EtOH (A.R., Sinopharm Chemical Reagent Co., Ltd., China) was of 99.7% purity. Stainless steel θ-mesh rings of Ø2 mm × 2 mm

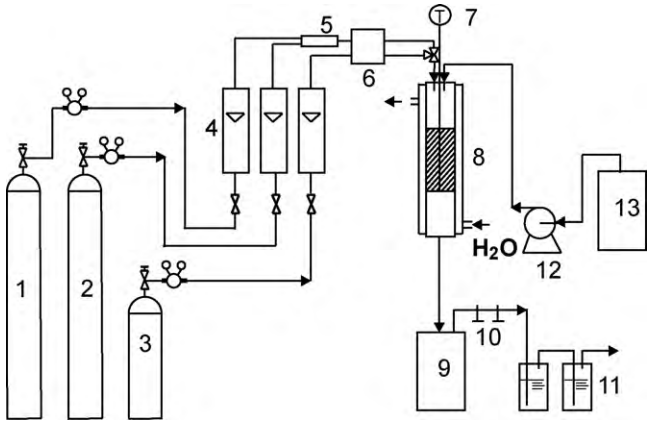

Fig. 1. Experimental setup (1, N_2; 2, O_2; 3, NO; 4, rotameter; 5, mixer; 6, preheater; 7, thermocouple; 8, tubular reactor; 9, cold trap; 10, gas sample; 11, NaOH solution; 12, metering pump; 13, EtOH).

with large specific surface areas ($3150\,m^2/m^3$) and a high porosity ($0.92\,m^3/m^3$) (Tianjin Beiyang Qiushi Apparatus Co., Ltd., Tianjin, in China) were purchased and used in this work.

2.2. Experimental setup and procedure

The experimental setup is schematically shown in Fig. 1. The tubular reactor, which was made of glass, was 300 mm long and 13 mm I.D. The θ-mesh rings were packed in the middle-upper part of the reactor. A stainless steel tube of 2 mm diameter with a thermocouple was embedded in the reactor to determine the temperature. The reactor temperature was controlled by a thermostatic circulating water bath, and the temperature difference along the reactor was less than 0.5 K. The gas feeding lines were equipped with a mixer and a heater. In each experimental run, an EtOH solution with a flow rate of 2.0 mL/min was introduced into the reactor for 30 min to ensure that the θ-mesh ring packing was fully wet. Then, NO, O_2, N_2, and EtOH were introduced into the reactor, where the products entered into the cold trap, while the non-condensable gas was passed through the alkali liquor to absorb NO_x, and then into the atmosphere. The concentrations of the products in the liquid sample in the cold trap and the non-condensable gas were analyzed separately.

2.3. Product analysis

The reaction products were analyzed by gas chromatography (Fuli 9790) equipped with a thermal conductivity detector (TCD). The external standard method was used. The water and EtOH concentrations in the liquid sample were analyzed by a Porpack-Q packed column. Hydrogen (99.999% pure, Sichuan Tianyi Science & Technology Co., Ltd., Sichuan, China) was used as the carrier gas with a flow rate of 30 mL/min at 0.3 MPa. The temperatures of injection, column, and detector were 110 °C, 90 °C, and 180 °C, respectively. The EN concentrations of the liquid sample and the non-condensable gas sample were analyzed by an oxydipropionylnitrile (ODPN) packed column and a 5A molecular sieve packed column, respectively.

2.4. Calculation and material balance

It is well known that analysis of O_2 in the non-condensable gas is difficult as there is NO in the non-condensable gas, which reacts easily with O_2. It was found that, in the trickle bed reactor, the regeneration reaction has very high selectivity and the reaction products are EN and water. On one hand, the boiling point of EN

is only 17 °C, and the EN produced in the reaction is difficult to analyze because a portion of the EN is in the cold trap and another portion of the EN is in the non-condensable gas. On the other hand, however, almost all of the water produced in the reaction is condensed to liquid form in the cold trap. Thus, the concentration of water can be accurately analyzed, and the conversion of O_2 can be calculated according to the following expression:

$$X_A = \frac{(\text{The mole of } H_2O \text{ produced in the reaction for } t \text{ min}) \times 1/2}{\text{The mole of } O_2 \text{ feed for } t \text{ min}} \times 100\% \quad (3)$$

To validate the reproducibility and the material balance of the experiment, each experiment was repeated three times under the same reaction conditions. The relative error was less than 1.7%. The relative error of the material mass between the inlet and the outlet of the reactor was found to be within 2.0%.

3. Results and discussion

3.1. Analysis of the regeneration reaction

It is well known that the regeneration reaction of EN involves the following reactions [6]:

$$2NO + O_2 \rightarrow 2NO_2 \quad (4)$$

$$NO_2 + NO \rightarrow N_2O_3 \quad (5)$$

$$C_2H_5OH + N_2O_3 \rightarrow C_2H_5ONO + HONO \quad (6)$$

$$C_2H_5OH + HONO \rightarrow C_2H_5ONO + H_2O \quad (7)$$

$$N_2O_3 + H_2O \rightarrow 2HONO \quad (8)$$

$$2NO_2 \leftrightarrow N_2O_4 \quad (9)$$

$$C_2H_5OH + N_2O_4 \rightarrow C_2H_5ONO + HNO_3 \quad (10)$$

$$N_2O_4 + H_2O \rightarrow HONO + HNO_3 \quad (11)$$

$$2C_2H_5OH + O_2 \rightarrow 2CH_3CHO + H_2O \quad (12)$$

$$C_2H_5OH + NO_2 \rightarrow CH_3CHO + NO + H_2O \quad (13)$$

From these reactions, it was found that the regeneration reaction is a very complicated process that involves many parallel and tandem reactions. Ethanal and nitric acid are also produced as byproducts. Because the regeneration reaction involves complicated elementary reactions, precise control of the reaction is required to increase the selectivity of EN and suppress the formation of nitric acid, which interrupts the desired reaction. To reduce the formation of byproducts, the concentration of N_2O_3 in the gas phase should be high. Therefore, a higher NO/O_2 molar ratio and a lower reaction pressure are necessary. Furthermore, the water in liquid phase should be maintained to as minimal as possible to inhibit the formation of nitric acid. The EtOH/NO molar ratio should also not be too small.

3.2. Effect of temperature

Fig. 2 shows that O_2 conversion increases with temperature in lower temperature ranges, but decreases when the temperature is higher than 323 K. The regeneration reaction for EN is an exothermic one ($\Delta_r H^{\theta}_{m,298\,K} = -121.11$ kJ/mol). The reaction is controlled by kinetic effects under 323 K, so the reaction rate increases with the temperature. However, the reaction is also controlled by thermodynamic effects, and O_2 conversion decreases at temperatures above 323 K. On the other hand, the solubilities of O_2 and NO in EtOH solution decrease with the increase in temperature, which is unfavorable to the reaction.

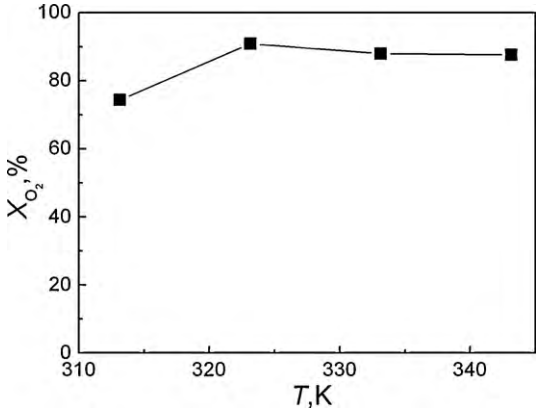

Fig. 2. Effect of temperature on O_2 conversion (reaction conditions: NO/O_2: 6:1 (mol); C_2H_5OH/NO: 3:1 (mol); N_2: 50% (vol). θ-mesh rings: 8 mL).

3.3. Effect of NO/O_2 molar ratio

It is shown, in Fig. 3, that O_2 conversion increases with the NO/O_2 molar ratio. According to the analysis of the reaction, a large amount of NO in the gas phase is necessary to reduce the formation of byproducts. O_2 should be fully consumed in the regeneration reaction because the catalyst used in the coupling reaction in the Ube process is easily deactivated by O_2. Therefore, the NO/O_2 molar ratio must be higher than the stoichiometric ratio 4:1. Hence, an NO/O_2 molar ratio of 6:1 is suitable for the reaction.

3.4. Effect of EtOH/NO molar ratio

The changes in O_2 conversion with EtOH/NO molar ratios are listed in Fig. 4. In these experiments, the gas flow rates of O_2, NO, and N_2 were kept constant, while the feed flow rate of EtOH was varied. O_2 conversion increases significantly from 71.68% to 85.05% as the EtOH/NO molar ratio increases from 2.0 to 3.0, but increases minimally as the EtOH/NO molar ratio is further increased to above 3.0. The gas hourly space velocity (GHSV) in these experiments remains constant because the gas flow rates are fixed. Thus, the increase in O_2 conversion means that the reaction rate increases. The above results indicate that, on the one hand, the regeneration reaction may change from liquid film-controlling to gas film-controlling when the EtOH/NO molar ratio is higher than 3.0. On the other hand, in the regeneration reaction, EtOH not only acts as a reagent, but also as a solvent and diluent of water. A larger EtOH/NO molar ratio is favorable to the regeneration reac-

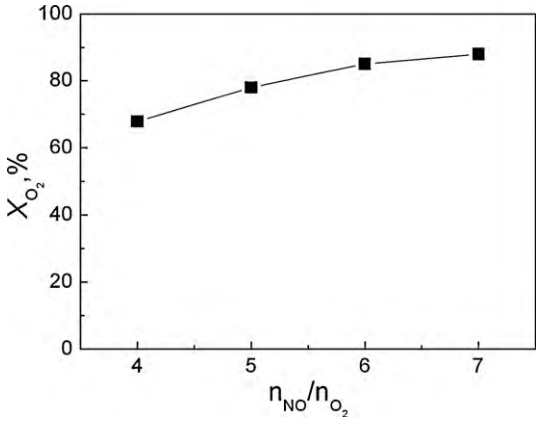

Fig. 3. Effect of NO/O_2 molar ratio on O_2 conversion (reaction conditions: T = 333 K; EtOH/NO: 3:1 (mol); N_2: 50% (vol). θ-mesh rings: 8 mL).

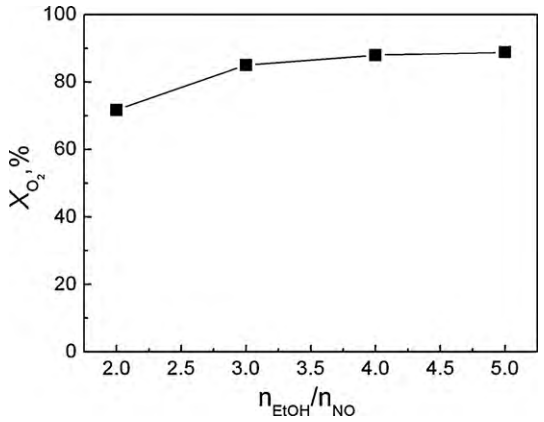

Fig. 4. Effect of EtOH/NO molar ratio on O_2 conversion (reaction conditions: T = 333 K; NO/O_2: 6:1 (mol); N_2: 50% (vol). θ-mesh rings: 8 mL).

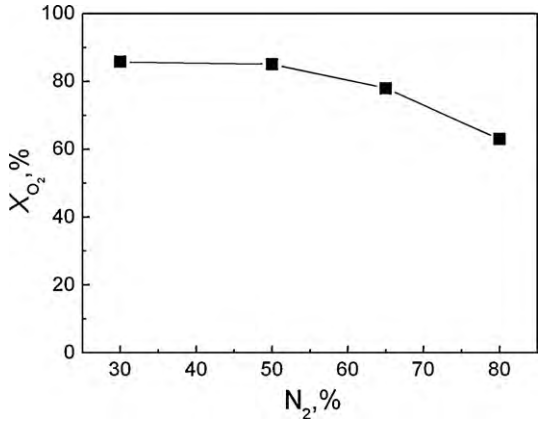

Fig. 5. Effect of N_2 volume fraction on O_2 conversion (reaction conditions: T = 333 K; NO/O_2: 6:1 (mol); EtOH/NO: 3:1 (mol). θ-mesh rings: 8 mL).

tion. Therefore, an EtOH/NO molar ratio of 3:1 would be suitable for the reaction.

3.5. Effect of N_2 volume fraction

O_2 conversion decreases slightly from 85.75% to 85.05% as the N_2 volume fraction initially increases from 30% to 50%. It then decreases more significantly from 85.05% to 62.98% when the N_2 volume fraction reaches 50% (Fig. 5). In these experiments, the feed flow rates of EtOH, NO, and O_2 were kept constant, while the feed flow rate of N_2 was varied. N_2 is favorable for the regeneration reaction because it promotes the diffusion of NO and O_2. However, excessive N_2 is unfavorable to the reaction due to the dilution of reactive gases. The LHSV in these experiments remained constant because the feed flow rate of EtOH was fixed. So, the change in O_2 conversion means that the reaction rate became slower under the experimental conditions. This result indicates that the regeneration reaction may change from liquid film-controlling to gas film-controlling when the N_2 volume fraction exceeds 50%. Therefore, an N_2 volume fraction of 30–50% would be suitable for the reaction.

3.6. Effect of LHSV

The effect of LHSV on the conversion of O_2 is also very important. As shown in Fig. 6, it is found that O_2 conversion decreases with LHSV. As expected, higher O_2 conversion can be achieved at lower LHSV, however, the space-time yield of EN would also decrease.

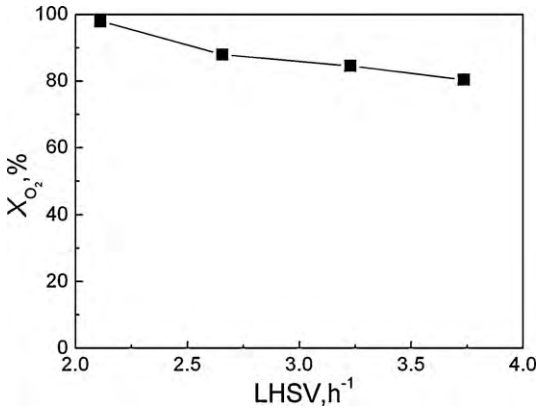

Fig. 6. Effect of LHSV on O_2 conversion (Reaction condition: T = 333 K; NO/O_2: 6:1 (mol); EtOH/NO: 3:1 (mol); N_2: 50% (vol). θ-mesh rings: 8 mL).

The O_2 conversion reached 90.9% under conditions of 333 K, NO/O_2 molar ratio of 6:1, EtOH/NO molar ratio of 3:1, N_2 volume fraction of 50%, and LHSV of 2.65 h^{-1}.

3.7. Kinetic model

3.7.1. Reaction rate

On the basis of the experiment results, the reaction kinetics of the regeneration reaction was studied. The experimental data of the reaction kinetics are listed in Table 1. The two-film model is used to establish the kinetic model due to its applicability and simplification. Some assumptions are made as follows: (1) The regeneration reaction is a fast reaction and takes place in the liquid film. (2) The concentration of EtOH in the liquid film is a constant and its saturated vapor pressure is neglected. (3) EN generated from the regeneration reaction rapidly diffuses into the gas phase. The power-law expression is usually used to calculate the intrinsic reaction rate of the gas–liquid reaction as it is accurate enough to estimate the reaction rates reported in the literature [15]. In this work, the intrinsic reaction rate of the regeneration reaction (2) is calculated by the following expression:

$$R_A = kC_AC_BC_C \tag{14}$$

where k is the rate constant, C_i is the molar concentration of component i in the liquid phase, and subscripts A, B and C denote O_2, NO, and EtOH, respectively.

The oxygen in the reaction is selected as a key component because it should be completely consumed in the regeneration reaction. When the resistance in the gas film is neglected, the mass transfer rate through the gas–liquid phase interface can be obtained as:

$$N_A|_{z=0} = k_{LA}\beta\frac{RTC_{AG}}{H_A} \tag{15}$$

$$\beta = \frac{\sqrt{D_{LA}kC_CRT(C_{BG}/H_B - (|\nu_B|D_{LA}/3D_{LB})(C_{AG}/H_A))}}{k_{LA}} \tag{16}$$

and the Hatta number, Ha, is defined as:

$$Ha = \frac{\sqrt{D_{LA}kC_{BG1}C_{CL}}}{k_{LA}} \tag{17}$$

Here, β is the enhancement factor, C_{AG} and C_{BG} are the molar concentrations of O_2 and NO in the gas phase, respectively, ν_B is the stoichiometric coefficient of NO, and k_{LA}, H_A, H_B, D_{LA}, and D_{LB} are the mass transfer coefficient of liquid film, the Henry's constants of O_2 and NO, and the diffusion coefficients of O_2 and NO in liquid, respectively. C_{BG1} and C_{CL} are the inlet concentration of NO and the liquid bulk concentration of EtOH, respectively.

Table 1
Experimental data of the reaction kinetics and calculated O_2 conversion (θ-rings: 6 mL).

No.	T (K)	F_{EtOH} (mol/h)	N_T (mol/h)	y_{NO} (%)	y_{O_2} (%)	y_{N_2} (%)	$X_{O_2}^{exp}$ (%)	$X_{O_2}^{cal}$ (%)	RE[a] (%)
1	313	0.366	0.2814	43.21	6.38	50.41	84.38	85.44	−1.26
2	313	0.444	0.3446	42.9	7.06	50.05	73.81	78.23	−5.99
3	313	0.516	0.3996	42.8	7.27	49.93	72.82	73.03	−0.29
4	313	0.444	0.2432	40.0	10.0	50.0	76.18	77.17	−1.30
5	313	0.612	0.3127	62.22	7.78	30.0	93.27	89.26	4.30
6	323	0.366	0.2814	43.21	6.38	50.41	90.89	91.94	−1.16
7	323	0.444	0.3446	42.9	7.06	50.05	90.44	86.17	4.72
8	323	0.516	0.3996	42.8	7.27	49.93	77.01	76.67	0.44
9	323	0.444	0.2432	40.0	10.0	50.0	79.91	82.92	−3.77
10	333	0.366	0.2814	43.21	6.38	50.41	87.96	90.69	−3.10
11	333	0.444	0.3446	42.9	7.06	50.05	84.56	84.41	0.18
12	333	0.516	0.3996	42.8	7.27	49.93	80.46	79.63	1.03
13	333	0.444	0.2432	40.0	10.0	50.0	76.06	75.60	0.60
14	343	0.366	0.2814	43.21	6.38	50.41	87.58	91.25	−4.19
15	343	0.444	0.3446	42.9	7.06	50.05	84.38	84.98	−0.71
16	343	0.516	0.3996	42.8	7.27	49.93	80.68	80.17	0.63
17	343	0.444	0.2432	40.0	10.0	50.0	77.57	79.69	−2.73
							F	2.01×10^4	
							$10 \times F_T$	44.9	

F_{EtOH}: EtOH feed flow rate; N_T: total gas feed flow rate.
[a] $RE = (X_{O_2}^{exp} - X_{O_2}^{cal})/X_{O_2}^{exp} \times 100\%$.

In Eq. (15), the O_2 conversion, X_A, is used instead of the component concentration, C_i, the mass transfer rate through the gas–liquid phase interface is expressed as follows:

$$N_A|_{z=0}a = \frac{(RT)^{3/2} a C_{AG1}\sqrt{D_{LA}kC_C}}{H_A} \times \frac{1-X_A}{(1+y_{A1}X_A\sigma_A)^{3/2}}\sqrt{\frac{C_{BG1}-(\nu_B/\nu_A)C_{AG1}X_A}{H_B} - \frac{|\nu_B|D_{LA}C_{AG1}(1-X_A)}{3D_{LB}H_A}} \quad (18)$$

where a is the effective gas–liquid interfacial area. C_{AG1}, y_{A1}, and σ_A are the inlet concentration of O_2, the initial molar fraction of O_2, and the expansion factor to O_2, respectively (the derivation of Eq. (18) is supplied in Appendix A).

The mass transfer coefficient of the liquid film and the effective gas–liquid interfacial area of the packed column with θ-mesh rings were determined by Luo et al. [16] using the method of CO_2 absorption into aqueous solutions of sodium hydroxide and are used in this work. The mass transfer coefficient is expressed as:

$$k_{LA} = 9.0 \times 10^{-5} L'^{0.45} \quad (19)$$

The effective gas–liquid interfacial area is expressed as:

$$a = 522.6 G'^{-0.0657} \quad (20)$$

The diffusion coefficients of O_2 and NO are calculated according to the following [17]:

$$D_{AB} = \frac{7.4 \times 10^{-8}(\alpha M_B)^{0.5} T}{\mu V_A^{0.6}} \quad (21)$$

The Henry's constants of O_2 and NO are given in the literature [18,19].

3.7.2. Reactor model

The plug flow model is used for the trickle bed reactor. The following expression for O_2 conversion, X_A, can be obtained through the gas phase mass balance:

$$\frac{dX_A}{dh} = P\sqrt{k}\frac{1-X_A}{(1+y_{A1}X_A\sigma_A)^{3/2}}\sqrt{Q+WX_A} \quad (22)$$

Here:

$$P = \frac{(RT)^{3/2} a \sqrt{D_{LA}C_C}}{H_A u_{OG1}\sqrt{3D_{LB}H_AH_B}} \quad (23)$$

$$Q = 3D_{LB}H_AC_{BG1} - |\nu_B|D_{LA}H_BC_{AG1} \quad (24)$$

$$W = |\nu_B|D_{LA}H_BC_{AG1} - \frac{3D_{LB}H_A|\nu_B|C_{AG1}}{|\nu_A|} \quad (25)$$

The total mass balance of gas phase and liquid phase is expressed as:

$$GC_{AG1}\frac{y_{A1}\sigma_A+1}{1+y_{A1}X_A\sigma_A}X_A = \frac{1}{|\nu_C|}L(C_{C1}-C_C) \quad (26)$$

The boundary conditions are:

$$h = 0, \quad X_A = 0, \quad C_C = C_{C1} \quad (27)$$

In Eq. (23), u_{OG1} is the gas inlet flow rate. In Eq. (26), C_{C1} is the inlet concentration of EtOH.

3.7.3. Kinetic parameters estimation

The reactor model, which is an initial value problem of the ordinary differential equations, is solved by the four-order Runge–Kutta method. The calculation program is compiled by MATLAB language. The rate constant is determined by minimizing the following expression:

$$\psi = \sum_{j=1}^{N}(X_{A,j}^{exp} - X_{A,j}^{cal})^2 \quad (28)$$

which is the squared sum of the residuals between the experimentally determined O_2 conversion, X_A^{exp}, and the model predicted, X_A^{cal}. Table 2 lists the rate constants that were determined by minimizing the residuals. The Hatta number and the enhancement factor

Table 2
The rate constant, the Hatta number and the enhancement factor at different temperature.

T (K)	k ($m^6/(mol^2\,s)$)	Ha	β
313	0.0126	87.4516	36.6777
323	0.0183	115.5759	45.8528
333	0.0221	143.5418	53.4014
343	0.0268	174.0201	59.9104

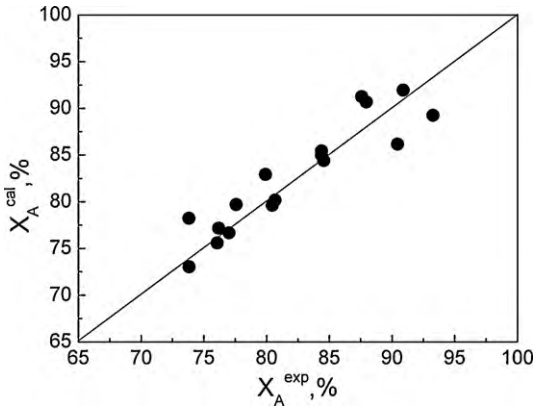

Fig. 7. Comparison of O_2 conversion calculated from the kinetics model with experimental data.

were calculated and are also listed in Table 2. The expression of the rate constant is obtained from the Arrhenius equation as:

$$k = \exp\left(4.121 - \frac{2645.7}{T}\right) \tag{29}$$

The correlation coefficient is 0.9755. An activation energy of 22.0 kJ/mol was obtained and it is consistent with the value of 22.9 kJ/mol in the literature [9]. As shown in Table 2, the $Ha \gg 3$, so the above assumption that the reaction is a fast one is acceptable. If the concentration of NO in the liquid film is assumed to be constant, the thickness of the reaction film, δ_R, and the thickness of the liquid film, δ_L, can be calculated as [20]:

$$\delta_R = \left[\frac{(m+1)D_{LA}}{2kC_BC_C(C_A^*)^{m-1}}\right]^{1/2} \tag{30}$$

$$\delta_L = Ha\delta_R \tag{31}$$

where $m = 1$, is the reaction order of O_2. At 313.15 K, δ_R and δ_L are 1.035×10^{-6} and 9.05×10^{-5} m, respectively. The result indicates that the regeneration reaction takes place in the liquid film because $\delta_R < \delta_L$.

With the kinetic parameters in this work, the outlet O_2 conversions were calculated and are listed in the ninth column of Table 1. The relative errors between the experimental- and model-predicted conversions are below 6%. These indicate that the calculated O_2 conversions are consistent with the experiments. Fig. 7 shows that the distributions of experimental and calculated values around the diagonal line are random. This suggests that the kinetics model described the experimental results well.

The results of statistical tests for the rate expression are reported in Table 1. As shown in the ninth column of Table 1, F is the ratio of the mean regression sum of squares to the mean residual sum of squares, which is calculated by:

$$F = \frac{\sum_{j=1}^{N}(X_{A,j}^{cal})^2/p}{\sum_{j=1}^{N}(X_{A,j}^{exp} - X_{A,j}^{cal})^2/(N-p)} \tag{32}$$

where N is the number of experimental runs and p is the number of parameters in the model. F_T represents the tabulated values corresponding to free degrees at the 5% level of degree of confidence [21]. Generally, a model is considered acceptable if $F > 10F_T$. The results listed in the ninth column of Table 1 imply that the F value is $2.01 \times 10^4 \gg 10\ F_T$ (=44.9). Thus, the kinetic model well represents the behaviors of the regeneration reaction.

4. Conclusions

It was found that the synthetic reaction of EN is a fast one and takes place in a liquid film. O_2 conversion increases with the NO/O_2 and EtOH/NO molar ratios, and decreases with the N_2 volume fraction and the LHSV. The effect of temperature on O_2 conversion was also discussed in detail. A kinetics model based on the two-film model was proposed and the plug flow model was developed for the gas–liquid phase reactor. It was shown that the kinetics model fits the experimental data very well at different temperatures and residence times.

Acknowledgements

We are thankful to Wuhuan Engineering Co., Ltd. for the financial support for this research, and Ms. Daying Han for kinetic experiments.

Appendix A. Derivation of Eq. (18)

Here the two-film model is used to establish the kinetic model. To obtain the mass transfer rate of A (O_2) through the gas–liquid phase interface, the mass balance for O_2 about a differential element of volume (the thickness is dZ and the area of the mass transfer is 1.0) in the liquid film is given as the following:

$$\left[-D_{LA}\frac{dC_A}{dZ}\right] - \left[-D_{LA}\left(\frac{dC_A}{dZ} + \frac{d^2C_A}{dZ^2}dZ\right)\right] - R_A \cdot dZ = 0 \tag{A.1}$$

Simplifying Eq. (A.1), we have:

$$D_{LA}\frac{d^2C_A}{dZ^2} = R_A = kC_AC_BC_C \tag{A.2}$$

Equating $\zeta = dC_A/dZ$, and introducing it into Eq. (A.2), we obtain:

$$\zeta\frac{d\zeta}{dC_A} = \frac{kC_C}{D_{LA}}C_AC_B \tag{A.3}$$

The boundary conditions of Eq. (A.3) are:

$$\begin{cases} Z = 0, & C_A = C_{Ai}, \quad C_B = C_{Bi}, \quad \dfrac{dC_C}{dZ} = 0 \\ Z = \delta_L, & C_A = 0, \quad C_B = C_{BL}, \quad \zeta = 0 \end{cases} \tag{A.4}$$

In the same way, we can obtain the following expression for B (NO):

$$D_{LB}\frac{d^2C_B}{dZ^2} = |\nu_B|R_A \tag{A.5}$$

So, we have

$$D_{LB}\frac{d^2C_B}{dZ^2} = |\nu_B|D_{LA}\frac{d^2C_A}{dZ^2} \tag{A.6}$$

We can obtain following expression through an integral operation for Eq. (A.6):

$$C_B = C_{Bi} - \frac{|\nu_B|D_{LA}}{D_{LB}}(C_{Ai} - C_A) \tag{A.7}$$

where C_{Ai} and C_{Bi} are the molar concentrations of O_2 and NO in the gas–liquid phase interface, respectively. Introducing Eq. (A.7) into Eq. (A.3), we have:

$$\zeta\frac{d\zeta}{dC_A} = \frac{kC_C}{D_{LA}}C_A\left[C_{Bi} - \frac{|\nu_B|D_{LA}}{D_{LB}}(C_{Ai} - C_A)\right] \tag{A.8}$$

We can obtain following expression through an integral operation for Eq. (A.8):

$$\zeta^2 = \frac{2kC_C}{D_{LA}}\left[\left(C_{Bi} - \frac{|\nu_B|D_{LA}}{D_{LB}}C_{Ai}\right)\frac{C_A^2}{2} + \frac{|\nu_B|D_{LA}}{D_{LB}} \times \frac{C_A^3}{3}\right] + C' \quad (A.9)$$

Introducing the boundary conditions (A.4) into Eq. (A.9), we have:

$$C' = 0 \quad (A.10)$$

Because $\zeta \leq 0$, we can obtain following expression:

$$\zeta = -\sqrt{\frac{2kC_C}{D_{LA}}\left[\left(C_{Bi} - \frac{|\nu_B|D_{LA}}{D_{LB}}C_{Ai}\right)\frac{C_A^2}{2} + \frac{|\nu_B|D_{LA}}{D_{LB}} \times \frac{C_A^3}{3}\right]} \quad (A.11)$$

The mass transfer rate of O_2 through the gas–liquid phase interface is:

$$N_A\big|_{Z=0} = -D_{LA}\left(\frac{dC_A}{dZ}\right)_{Z=0} = -D_{LA}(\zeta)_{Z=0} \quad (A.12)$$

Introducing Eq. (A.11) into Eq. (A.12), we have:

$$N_A\big|_{Z=0} = \left[\sqrt{D_{LA}kC_C\left(C_{Bi} - \frac{|\nu_B|D_{LA}}{3D_{LB}}C_{Ai}\right)}\right]C_{Ai} = k_{LA}\beta C_{Ai} \quad (A.13)$$

where:

$$\beta = \frac{\sqrt{D_{LA}kC_C(C_{Bi} - (|\nu_B|D_{LA}/3D_{LB})C_{Ai})}}{k_{LA}} \quad (A.14)$$

When the resistance in gas film is neglected, according to Henry's law and the ideal gas equation, we have:

$$C_{Ai} = \frac{p_A}{H_A} = \frac{RTC_{AG}}{H_A} \quad (A.15)$$

$$C_{Bi} = \frac{p_B}{H_A} = \frac{RTC_{BG}}{H_B} \quad (A.16)$$

where p_A and p_B are the partial pressures of O_2 and NO in the gas phase, respectively. Introducing Eqs. (A.15) and (A.16) into Eqs. (A.13) and (A.14) to eliminate the unknown interface concentrations C_{Ai} and C_{Bi}, we have:

$$N_A\big|_{Z=0} = k_{lA}\beta\frac{RTC_{AG}}{H_A} \quad (A.17)$$

$$\beta = \frac{\sqrt{D_{LA}kC_CRT(C_{BG}/H_B - (|\nu_B|D_{LA}/3D_{LB})(C_{AG}/H_A))}}{k_{LA}} \quad (A.18)$$

Eqs. (A.17) and (A.18) are simply Eq. (15) and Eq. (16), respectively. According to the definition of O_2 conversion, X_A, we have:

$$C_{AG} = \frac{C_{AG1}(1 - X_A)}{1 + y_{A1}X_A\sigma_A} \quad (A.19)$$

$$C_{BG} = \frac{C_{BG1} - (\nu_B/\nu_A)C_{AG1}X_A}{1 + y_{A1}X_A\sigma_A} \quad (A.20)$$

Finally, introducing Eqs. (A.19) and (A.20) into Eqs. (A.17) and (A.18), we have:

$$N_A|_{z=0}a = \frac{(RT)^{3/2}aC_{AG1}\sqrt{D_{LA}kC_C}}{H_A} \times \frac{1 - X_A}{(1 + y_{A1}X_A\sigma_A)^{3/2}}\sqrt{\frac{C_{BG1} - (\nu_B/\nu_A)C_{AG1}X_A}{H_B} - \frac{|\nu_B|D_{LA}C_{AG1}(1 - X_A)}{3D_{LB}H_A}} \quad (A.21)$$

Here, Eq. (A.21) is simply Eq. (18).

References

[1] S.I. Uchiumi, K. Ataka, T. Matsuzaki, Oxidative reactions by a palladium-alkyl nitrite system, J. Organoment. Chem. 576 (1999) 279–289.
[2] T. Matsuzaki, A. Nakamura, Dimethyl carbonate synthesis and other oxidative reactions using alkyl nitrites, Catal. Surveys Jpn. 1 (1997) 77–88.
[3] F.E. Celik, T.J. Kim, A.T. Bell, Vapor-phase carbonylation of dimethoxymethane over H-Faujasit, Angew. Chem. Int. Ed. 48 (2009) 1–4.
[4] X.Z. Jiang, Y.H. Sua, B.J. Lee, S.H. Chien, A study on the synthesis of diethyl oxalate over Pd/a-Al_2O_3 catalysts, Appl. Catal. A: Gen. 211 (2001) 47–51.
[5] L.F. Chen, P.J. Guo, M.H. Qiao, S.R. Yan, H.X. Li, W. Shen, H.L. Xu, K.N. Fan, Cu/SiO_2 catalysts prepared by the ammonia-evaporation method: texture, structure, and catalytic performance in hydrogenation of dimethyl oxalate to ethylene glycol, J. Catal. 257 (2008) 172–180.
[6] Y.H. Su, J.M. Ji, X.Z. Jiang, S.H. Zhou, A study on the regeneration ethyl nitrite, Chem. Reaction Eng. Technol. (in Chinese) 16 (2000) 45–49.
[7] K. Nishihira, S. Tanaka, S. Yoshida, Process for producing alkyl nitrite, EP Patent 0,911,316 A2 (1999).
[8] J. Doumaux, R. Arthur, M. James, P. Joseph, M. John, Preparation of nitrite esters, US Patent 4,353,843 (1982).
[9] J.W. Chen, G.H. Xu, Z.H. Li, H.F. Chen, kinetics of regeneration reaction for CO coupling, J. Chem. Ind. Eng. (China) (in Chinese) 44 (1993) 66–72.
[10] Z.C. Hu, D.X. Yin, C.Y. He, X.B. Ma, Z.H. Li, New technique for ethyl nitrite regeneration, Chem. Ind. Eng. (in Chinese) 25 (2008) 112–115.
[11] B.W. van Hasselt, H.P.A. Calis, S.T. Sie, C.M. van den Bleek, Gas–liquid mass transfer characteristics of the three-levels-of porosity reactor, Chem. Eng. Sci. 56 (2001) 531–536.
[12] R.D. Vas Bhat, J.A.M. Kuipers, G.F. Versteeg, Mass transfer with complex chemical reactions in gas–liquid systems: two-step reversible reactions with unit stoichiometric and kinetic orders, Chem. Eng. J. 76 (2000) 127–152.
[13] C. Fleischer, S. Becker, G. Eigenberger, Detailed modeling of the chemisorption of CO_2 into NaOH in a bubble column, Chem. Eng. Sci. 51 (1996) 1715–1724.
[14] X. Huang, A. Varma, M.J. McCready, Heat transfer characterization of gas–liquid flows in a trickle-bed, Chem. Eng. Sci. 59 (2004) 3767–3776.
[15] R.D. Vas Bhat, W.P.M. van Swaaij, J.A.M. Kuipers, G.F. Versteeg, Mass transfer with complex chemical reaction in gas–liquid systems-I. Consecutive reversible reactions with equal diffusivities, Chem. Eng. Sci. 54 (1999) 121–136.
[16] P.C. Luo, Z.B. Zhang, Z. Jiao, Z.X. Wang, Investigation in the design of a CO_2 cleaner system by using aqueous solutions of monoethanolamine and diethanolamine, Ind. Eng. Chem. Res. 42 (2003) 4861–4866.
[17] C.R. Wilke, P. Chang, Correlation of diffusion coefficients in dilute solutions, AIChE J. 1 (1955) 264–270.
[18] R. Battino, Solubility Data Series, vol. 7, Oxygen and Ozone, Pergamon Press, Oxford, 1981, p. 274.
[19] C.L. Young, Solubility Data Series, vol. 8, Oxides of Nitrogen, Pergamon Press, Oxford, 1981, p. 343.
[20] X.Z. Jiang, Theory and Application Basis of Gas–Liquid Reaction (in Chinese), Hydrocarbon Processing Press, Peking, 1989, p. 129.
[21] J.L. Ayastuy, M.A. Gutierrez-Ortiz, J.A. Gonzalez-Marcos, A. Aranzabal, J.R. Gonzalez-Velasco, Kinetics of the low-temperature WGS reaction over a CuO/ZnO/Al_2O_3 catalyst, Ind. Eng. Chem. Res. 44 (2005) 41–50.